Published in final edited form as:
J Comp Neurol. 2013 May 1; 521(7): 1683–1696. doi:10.1002/cne.23257.

Commissural Axons of the Mouse Cochlear Nucleus

M. Christian Brown[1,2], **Marie Drottar**[1], **Thane E. Benson**[1], and **Keith Darrow**[1,3]

[1]Eaton-Peabody Laboratory, Massachusetts Eye and Ear Infirmary, Harvard Medical School, Boston, MA 02114, USA

[2]Department of Otology and Laryngology, Harvard Medical School, Boston, MA 02114, USA

[3]Department of Communication Sciences and Disorders, Worcester State University

Abstract

The axons of commissural neurons that project from one cochlear nucleus to the other were studied after labeling with anterograde tracer. Injections were made into the dorsal subdivision of the cochlear nucleus in order to restrict labeling only to the group of commissural neurons that gave off collaterals to, or were located in, this subdivision. The number of labeled commissural axons in each injection was correlated with the number of labeled radiate multipolar neurons, suggesting radiate neurons as the predominant origin of the axons. The radiate commissural axons are thick and myelinated, and they exit the dorsal acoustic stria of the injected cochlear nucleus to cross the brainstem in the dorsal half, near the crossing position of the olivocochlear bundle. They enter the opposite cochlear nucleus via the dorsal and ventral acoustic stria and at its medial border. Reconstructions of single axons demonstrate that terminations are mostly in the core and typically within a single subdivision of the cochlear nucleus. Extents of termination range from narrow to broad along both the dorso-ventral (i.e. tonotopic) and rostro-caudal dimensions. In the electron microscope, labeled swellings form synapses that are symmetric (in that there is little postsynaptic density), a characteristic of inhibitory synapses. Our labeled axons do not appear to include excitatory commissural axons that end in edge regions of the nucleus. Radiate commissural axons could mediate the broad-band inhibition observed in responses to contralateral sound, and they may balance input from the two ears on a quick time course.

Keywords

auditory brainstem; inhibitory synapse; glycine; electron microscopy; binaural balance; multipolar cell

INTRODUCTION

Commissural pathways connect the right and left cochlear nuclei. As shown by retrograde labeling, commissural axons arise from neurons located mostly in the ventral cochlear nucleus (VCN) and in some cases in the deep portions of the dorsal cochlear nucleus (DCN) (Adams and Warr, 1976; Wenthold, 1987; Cant and Gaston, 1982; Shore et al., 1992; Alibardi, 1998, 2000; Doucet et al., 2009; Zhou et al., 2010). Commissural neurons are a subset of cochlear nucleus (CN) multipolar (stellate) cells, a group of cells that shows considerable variation in size and structure (Osen, 1969; Brawer et al., 1974; Doucet and Ryugo, 2006). Two major groups of multipolar cells have been separated according to anatomical and physiological criteria. The first group has several designations: type II cells

Correspondence to: M. Christian Brown, Eaton-Peabody Laboratory, Massachusetts Eye and Ear Infirmary, Boston, MA, USA. Phone: 617-573-3875. Fax: 617-720-4408. Chris_Brown@meei.harvard.edu.

due to dense innervation of their soma (Cant, 1981; Alibardi, 1998), D cells because their axon projects in the dorsal direction (Oertel et al., 1990), radiate cells due to their radiating dendrites (Oertel et al., 1990; Doucet and Ryugo, 1997), and onset choppers because of their pattern of response to sound (Rhode and Smith, 1986; Arnott et al., 2004). These large neurons are glycinergic (Wenthold, 1987; Alibardi, 1998, 2000; Kolston et al., 1992; Doucet et al., 1999) and their endings have inhibitory morphology (Smith et al., 2005). Many of these multipolar cells project commissurally (Cant and Gaston, 1982; Alibardi, 1998, 2000; Smith et al., 2005; Doucet et al., 2009) although some cells classified as radiate cells do not (Doucet and Ryugo, 2006).

A second group of multipolar cells, designated type I cells/T cells/planar cells/chopper units have different characteristics than the group described above and are primarily considered to be excitatory (reviewed by Oertel et al., 2011). These cells generally project to the superior olivary complex and inferior colliculus (Oliver, 1987; Schofield and Cant, 1996; Doucet and Ryugo, 2003; Darrow et al., 2012; reviewed by Doucet and Ryugo, 2006). Some excitatory multipolar cells project commissurally (Shore et al., 1992; Schofield and Cant, 1996; Alibardi, 1998, 2000; Doucet et al., 2009; Zhou et al., 2010). Although it is not clear whether they belong to the type I cells/T cells/planar cells/chopper units because of this atypical projection, most of these commissural multipolar neurons do have sparse innervation of their somata and thus have been termed “type I cells” (Doucet et al., 2009). Their somata are smaller than type II cells and they have a range of sizes (Shore et al., 1992; Schofield and Cant, 1996; Doucet et al., 2009). Some of them may be part of an additional group of multipolar cells called “small cells” (Osen, 1969; Brawer et al., 1974; Doucet and Ryugo, 2006).

The approach of the present work is to study commissural neurons that are labeled by injections into the DCN. Although most commissural neurons are located in the VCN, some of them give off collateral branches to the DCN (Doucet and Ryugo, 2006). Our study targets this subgroup, and we provide evidence that this approach specifically labels the inhibitory, but not the excitatory, commissural neurons described above. Furthermore, we provide information about the axonal trajectories and terminations of these neurons. Commissural axons are known to project dorsally via the CN’s dorsal acoustic stria, after which they traverse the midline (Cant and Gaston, 1982; Arnott et al., 2004; Smith et al., 2005). They cross the brainstem’s midline at the level of the genu of the facial nerve, which is the approximate crossing position of another auditory pathway, the olivocochlear bundle (Rasmussen, 1946; Brown, 1993). Lesions of that bundle have been used to study its function (Dewson, 1968; Rajan and Johnstone, 1989; Irving et al., 2011), and here we investigate the relationship of the olivocochlear bundle’s location to that of the commissural axons to infer whether the latter are sometimes interrupted by the same lesions. When the axons arrive at the opposite CN, commissural terminations are reported both in its central core (Cant and Gaston, 1982) and in edge regions (Zhou et al., 2010). However, partly due to the problem of fading of reaction product over long distances, existing knowledge is unclear about whether single axons innervate one or more of the CN subdivisions and whether single axons terminate broadly or narrowly along important dimensions of the CN such as the tonotopic axis. We chose to examine commissural axons in mice, which have small brainstems compared to cats and larger rodents used previously. This choice has enabled us to trace the axonal trajectories and reconstruct terminations of individual commissural axons on the opposite side of the brainstem. The radiate commissural system labeled by DCN injections arises in the core of the CN and projects thick, myelinated axons across the brainstem. These axons usually terminate within a single CN subdivision, but within that subdivision their terminations are widespread within its core region.

MATERIALS AND METHODS

All experimental procedures on CBA/CaJ mice were performed in accordance with the National Institutes of Health guidelines for the care and use of laboratory animals as well as approved animal care and use protocols at the Massachusetts Eye & Ear Infirmary. Some of the mice were also used in another study (Darrow et al., 2012). Mice were aged 8 – 12 weeks, weighing 20 – 26 g., and of either sex. Following anesthesia (xylazine 20 mg/kg i.p. and ketamine 100 mg/kg i.p.) the mouse was held in a Kopf small-animal stereotaxic apparatus by snout clamp. The skin overlaying the skull was incised and retracted to reveal the bregma and lambda sutures. A craniotomy of the left posterior-ventral skull surface was performed using rongeurs. Partial cerebellar aspiration (of the left hemisphere) exposed the dorsal surface of the brainstem. The surface landmarks and the ampulla of the superior semicircular canal were used to identify the DCN.

In each animal, a micropipette (diam. 10 – 40 μm) was filled with a 10% solution of the anterograde tracer biotinylated dextran-amine (BDA, MW 10,000; Molecular Probes) and inserted into the DCN on the left side. The BDA was injected by current applied to the pipette (+ 5 μA with an on/off duty cycle of 7 s for 8–12 min.). Immediately following injection, the scalp was sutured and the animal was placed in a padded cage with moist food and a gel-pack. Animals were allowed to survive 5 days post-injection.

Animals for study with the light microscope were perfused intracardially with physiologic saline followed by 4% paraformaldehyde in 0.05 M phosphate buffer (pH 7.2). The brainstems were extracted, post-fixed 2 hours, cryoprotected in 30% sucrose overnight, frozen and cut on a sliding microtome at 80 μm in the transverse plane. Free-floating sections for the single-injection cases were treated with 0.5% hydrogen peroxide, washed in phosphate buffer and incubated in ABC (Vector Labs Vectastain ABC kit PK 4000 with 0.3% Triton X-100) overnight at room temperature. Color development was achieved with DAB, 1% nickel ammonium sulfate, 1% cobalt chloride, and 1% DMSO. Sections were mounted on subbed slides and coverslipped. In 3 of the 15 animals studied in detail, a second injection of Fluorogold had been made into the cochlea (to label olivocochlear neurons for a separate study). In these cases, the BDA processing step was preceded by an anti-FG processing step; this step did not interfere with the BDA labeling. In our 42 injections processed for light microscopy, 15 had no labeling in the opposite CN even though there was abundant labeling elsewhere in the brainstem, while 27 had labeling in the opposite CN (15 of these cases were studied in detail).

Animals for possible study with the electron microscope (an additional 10 animals, of which 2 were used for electron microscopy) were perfused with physiologic saline followed by 0.5% paraformaldehyde and 1% glutaraldehyde in 0.1 M cacodylate buffer. This was followed by 0.5% paraformaldehyde and 3% glutaraldehyde in buffer. After an hour in the skull, the brainstems were removed and fixed an additional hour before immersion in buffered saline overnight. The brainstems were then embedded in gelatin-albumin, sectioned with a vibratome (80 μm), and processed for BDA as above. Select sections were post-fixed with 1% OsO_4, and then 1% uranyl acetate. The sections were dehydrated with methanol, infiltrated with epoxy, and flat-embedded between two transparent sheets of Aclar (Pro Plastics, Wall, NJ). In this material, light microscopy was first used to study labeled axons and then selected pieces were cut out, mounted on a block, and sectioned with an ultramicrotome (80 nm). Periodically during sectioning, the block was removed and examined with the light microscope to determine which labeled axons remained vs. which had been sectioned. Sections were examined using an electron microscope with magnification of 5,800x – 34,000x.

We restricted our investigation to cases in which the injection site was contained within the DCN; those where it encroached into the underlying restiform body, the VCN, or other nuclei were not used. In the studied cases, a light microscope fitted with a drawing tube was used to draw courses of individual axons that could be separated from the other labeled fibers. To follow the labeled axon from the upper edge of a section to the lower edge of the adjacent section, the position (relative to structures and other labeled fibers), thickness and darkness of the axon were used. Axonal diameters were measured from scanned camera-lucida drawings made with the light microscope. Using ImageJ (Abramoff et al. 2004), the area of the labeled axon was measured and divided by the path length (about 100 μm) to obtain the average diameter.

For the axon swellings, terminal swellings were defined as occurring at the tips of branches, and en passant swellings were defined as either twice the diameter of the fiber or branch or on stalks less than 5 μm long. The dorso-ventral distribution of swellings was plotted by assigning the swellings to 10 linearly spaced bins oriented along the approximate tonotopic axis of each section (ventral to dorsal for the VCN and ventro-lateral to dorso-medial for the DCN). Separately, the rostro-caudal distribution of swellings was plotted using the swellings within each transverse section (80 μm thickness). From these plots, the “60% extents” of each individual axon’s swellings were quantified by starting at the bin or section with the highest number of swellings and moving in both directions (or only one direction if bins or sections with zero counts were encountered in the other direction) until achieving 60% of the total (linear interpolation was used between each section).

Three additional mouse brainstems processed for acetylcholinesterase were used to locate the position of the midline crossing position of the olivocochlear bundle. These mice were not injected with tracer. Stains for acetylcholinesterase were by the Koelle indirect method (Koelle and Friedenwald, 1949 but modified as in Osen et al., 1984). First, sections were incubated for 30 min in acetylthiocholine medium (0.072 g ethopropazine, 1.156 g acetylthiocholine iodide, 0.750 g glycine, 0.5 g copper sulfate, and 6.8 g sodium acetate in 1000 ml distilled water, titrated to pH 5.0), rinsed in distilled water, incubated for 1 min in 4% sodium sulfide solution (pH 7.8), rinsed, incubated for 30 s in 1% silver nitrate, and rinsed again. The sections were dried onto subbed slides and then dehydrated and counterstained with neutral red.

RESULTS

Origin and Course of Labeled Axons

Focal injections of biotinylated dextran amine into the DCN label “radiate cells” (Fig. 1A, white arrow) located in the core of the VCN. These large neurons (diam. 20–26.5 μm) have dendrites that radiate in different directions and travel for long distances from the soma. The number of labeled radiate cells was small (range 0 to 30 per injection in counts from 13 injections). They typically occur outside the dense band of more abundant labeling of medium-sized multipolar neurons known as “planar cells” (Fig. 1A, black arrow) but a few are visible within the band (Doucet et al. 1999). The projections of planar cells, which exit the CN ventrally toward the superior olivary complex, are described elsewhere (Doucet and Ryugo, 2003; Darrow et al., 2012). Present results focus on the dorsal projections of commissural neurons that terminate in the contralateral CN (Fig. 2). Correlational analysis of the number of labeled radiate cells and the number of labeled commissural axons (Fig. 1B, R = .971) suggests radiate neurons as the origin for the axons; thus, this system will be referred to as “radiate commissural” neurons. In our counts, radiate neurons outnumber commissural axons by a ratio of approximately 3:1 (note different scales on axes of Fig. 1B). This non-uniform ratio may be due to radiate neurons that are not commissural (Doucet and Ryugo, 2006) but our data cannot exclude the possibility that it results from reaction product

that was too faint to discern in some axons. Finally, due to the fact that the reaction product at the injection site obscures labeling of DCN neurons (Fig. 1C), we do not know how many commissural neurons that originate in the DCN were labeled (Zhou et al., 2010).

The radiate commissural axons exit the injected DCN via the dorsal acoustic stria (das, Fig. 2) along with many other labeled fibers. Almost all of these fibers cross the midline in a diffuse swath and then run in the lateral lemniscus (LL, Fig. 2), eventually terminating in the inferior colliculus (not illustrated). The commissural axons peel off from the majority to innervate the opposite CN, which they enter via its dorsal or ventral acoustic striae or via an intermediate position at its medial border (das, vas, mb, Fig. 2, right side). There were no axons that innervated the opposite CN and then proceeded further toward the nuclei of the lateral lemniscus or inferior colliculus, in agreement with Schofield and Cant (1996b).

Some radiate commissural axons could be isolated and traced as individual axons in their entirety from the injected side to the opposite CN. The courses of these single axons are indicated on a composite brainstem outline in Figure 3. After exiting the injection site (left), the labeled axons project across the brainstem in its dorsal half. With respect to the ventral and dorsal edges of the brainstem, the average depth of axons crossing the midline is 62.9% (range 51 to 78, re: ventral edge). As a group, these axons are more ventral and much more spread out than axons in the nearby olivocochlear bundle (OCB, gray lines at dorsal midline on Fig. 3). In acetylcholinesterase-stained material, the OCB crosses the midline at an average position of 75.2% (range 73 to 79, re: ventral edge). Rostro-caudally, though, the crossings of the two fiber groups are very similar and they are both just rostral to the middle of the genu of cranial nerve VII (avg. midline position of commissural axons was 154 μm rostral to the genu (range 80 to 400 μm), and avg. OCB crossing was 80 μm rostral to the genu). The distances that these axons traveled, beginning at the left acoustic stria and ending at the estimated center of terminations in the right CN, averaged 5.0 mm (range 4.3 – 5.7 mm, n=14).

Radiate commissural axons have diameters that are thicker than auditory nerve fibers. Commissural axons averaged 2.1 μm diam. (10 labeled axons measured just before entry into the opposite CN), whereas auditory nerve fibers averaged 1.6 μm diam. (10 labeled fibers measured in the auditory nerve stump in the same injections, significantly different by t-test, P =.009). The thickest commissural axons tend to enter the opposite CN through the middle access route. Some commissural axons branch just before entering the opposite CN, at which point the branches usually become thinner than the parent axons. The labeled commissural axons have periodic constrictions along their course that are interpreted as nodes of Ranvier (Liberman and Oliver, 1984). The nodes persist even after several major branches have been formed within the CN. Most axons directed all their branches to the opposite CN, but one commissural axon gave off a branch to the superior olivary complex opposite the injection site (Fig. 3) and another (not included in Figure 3 because it was only partially reconstructed) gave off a thin branch that ran caudally through the spinal vestibular nucleus. Other caudally-running thin branches were observed in our material but we could not link them to their fibers of origin.

Terminations of Labeled Axons

Terminations of individual axons were reconstructed from injection cases that had small numbers of labeled axons so that each axon's terminations could be followed unambiguously. Individual axons usually terminated within a single CN subdivision. For a total of 34 axons from 15 injections in which the terminations could be assigned, 30 (88%) terminated in one subdivision, although three of these axons did have few (< 10%) of their endings in an adjacent subdivision. Of the total, 17 axons (50%) terminated in AVCN, 4 axons (12%) terminated in PVCN, and 9 axons (26%) terminated in DCN. Finally, of the 34

axons, 4 axons terminated about equally in two subdivisions: 2 axons (6%) terminated in AVCN and DCN, 1 axon (3%) terminated in DCN and PVCN, and 1 axon (3%) terminated in AVCN and PVCN. Axons tended to take the shortest route to the subdivision of terminations but there were exceptions: Some axons that terminated in DCN entered via the ventral acoustic stria (orange fiber, Fig. 3).

Within the subdivision of termination, an individual axon's branching can be extensive (Fig. 4). A total of 15 axons could be reconstructed to all their branches and swellings. One example axon that entered ventrally in AVCN (Fig. 4A) began branching immediately and continued to branch along its course to almost the dorsal edge of the nucleus. Another axon entered at the medial border of PVCN and terminated over a wide swath of this subdivision (Fig. 4B). A third axon passed through part of PVCN, gave off a few branches there, and then terminated through a large ventral-to-dorsal extent in DCN (Fig. 4C). Swellings were frequent along the branches and at their tips (Fig. 4C, arrowhead). En passant swellings were the most numerous. The axon of Figure 4A had 588 en passant vs. 120 terminal swellings. The axon of Figure 4B had 210 en passant vs. 61 terminal, and the axon of Figure 4C had 247 en passant vs. 93 terminal swellings. Combining the two types of swellings, the average number of swellings per axon was 250.3 (range 60 – 340 for 15 axons). Some of the swellings extended to edge regions such as the granule cell lamina (Fig. 4B, C, arrows).

The terminations of single axons were quantified in the dorso-ventral (tonotopic) and rostro-caudal dimensions (Fig. 4, graphs below each axon). En passant and terminal swellings were combined for this analysis. The dorso-ventral dimension is approximately the tonotopic axis for the CN (Osen, 1970; Bourk et al., 1981). Here, the full extent was divided into 10 equally spaced bins (see example bins in Fig. 5) and the percentage of swellings was plotted within each bin. The terminations had a range of extents. The three axons illustrated had swellings in most or all bins. Others had their swellings concentrated within a smaller number of bins. The extent of termination was quantified by calculating the number of bins in which 60% of the swellings were formed. This "60% extent" is given in the numbers on each plot. For example, the three individual axons illustrated in Figure 4 have a 60% extent of 3.9, 4.0, and 3.0 bins. For the 15 reconstructed axons, the average 60% extent was 2.6 bins (range 1.0 – 5.0 bins). In the rostro-caudal dimension, where terminations were measured as a function of section number, the 60% extent averaged 2.5 sections (range 1 – 3.9 sections). Specifically, the rostro-caudal extents of the three individual axons illustrated in Figure 4 were 1.8, 2.0, and 3.3 sections. Individual axon extents were compared in the two dimensions, but there was little correlation (R=0.18, not shown).

The terminations of anterogradely labeled commissural axons were also analyzed in injection cases that had abundant labeling in the opposite CN. One example, KND 169, is shown in atlas drawings in Figure 5 (and a second case, KND 228, was shown in Fig. 2). In the VCN, the terminations are mainly to the core of the nucleus with a few endings around the edges. The labeling is heaviest in the middle portion of AVCN, with less labeling in the PVCN. The ventral parts of AVCN and PVCN have few endings. Caudally in PVCN and rostrally in AVCN, the labeling drops off. There is a moderate amount of labeling in the DCN.

The terminations of three cases with abundant label were analyzed quantitatively in the dorso-ventral dimension. The VCN results (Fig. 6A) indicate that the average number of swellings is small in ventral locations (left side of graph) and rises in the middle regions continuing to rise somewhat for more dorsal locations. Along the DCN's dorso-ventral position (Fig. 6B), the average termination was more even. The overall pattern of labeling of radiate cells in these cases (Fig. 6A, inset) was also even, however, there were no cells at extreme ventral and dorsal positions (bins 1 and 10). Rostro-caudally, the distribution of

opposite-side terminations was analyzed by plotting the numbers of swellings in each section. The results (Fig. 6B) indicate low numbers of swellings in PVCN, with increasing numbers toward the middle and rostral portions of AVCN and then dropping off for the extreme rostral end of AVCN. In DCN, the rostro-caudal distribution also rises for more rostral locations, but drops off less at the extreme rostral edge. Overall, the middle and dorso-rostral parts of the CN, especially the AVCN, receive the densest projections.

Labeled Endings Form Synapses

Commissural axon terminations in the core of AVCN on the side opposite the injection were chosen for examintion with the electron microscope. Within the CN, commissural axons are myelinated (Fig. 7C). The branches of the axons chosen for examination formed frequent swellings that were first documented using the light microscope. For example, for the two labeled branches in the field of Figure 7A, we counted a total of 22 en passant and 6 terminal swellings of which most were in neuropil (19 of these en passant and 3 of these terminal swellings), with the 6 others appearing to contact cell bodies. Material subsequently examined in the electron microscope demonstrated that synapses were formed by the labeled swellings. All 18 synapses from the two animals examined were symmetric in that there was minimal postsynaptic density (Fig. 7B, D, E). They were generally straight and ranged in length from 0.5 to 0.75 μm. The shape of the synaptic vesicles was difficult to estimate in most cases due to reaction product decoration. In two synapses, however, the vesicles were clearly pleomorphic (one shown Fig. 7D). The synaptic terminals also contained coated vesicles.

The most common targets of the labeled synaptic terminals were dendrites (15 of 18 targets, Fig. 7B). The dendrites ranged in diameter from 0.5 to 1.25 μm. They could not be followed far enough to determine their origin. The other three targets were somata of AVCN principal cells. The first soma was contacted by a terminal swelling (Fig. 7A, solid arrow). This soma was oblong and its long dimension was 20 μm; it had several dendrites so we designate it as a multipolar cell (MC) on the figure. It was faintly labeled itself, suggesting that it was a retrogradely labeled commissural cell (as described previously). The synaptic terminal (Fig. 7C, solid arrow) forms a synapse onto the soma that is illustrated at high magnification in Figure 7D. This synaptic terminal and others that were unlabeled gave the soma a sparse coverage (20% membrane coverage, inset to Fig. 7C), which would be typical of type I multipolar cells (Cant, 1981; Doucet et al., 2009). In contrast, two other neurons (not illustrated) were different in that they received dense coverage of their somata (60% and 77% coverage). One of them could not be identified, but the third soma received two unlabeled synaptic terminals with endbulb-like morphology. The terminals were large (3.1 and 3.6 μm long) and they abutted the cell in segments (separated by glial intrusions) where they formed multiple, curved, asymmetric synapses. These observations suggest that this third neuron was a bushy cell (Ryugo et al. 1996).

Labeling of Somata in the Opposite Cochlear Nucleus

In some of our animals, there were a few labeled somata in the opposite CN (Fig. 7A). We found a total of 58 labeled neurons, from 1–16 per animal, in 14 out of 52 animals. These neurons are interpreted as being retrogradely labeled and projecting commissural axons to the injection site. They are large radiate multipolar cells similar in morphology to those described on the injected side (Fig. 1A). They were located in core regions of the posteroventral and anteroventral subdivisions (PVCN, AVCN). We observed a few of their faintly labeled axons in the commissural bundle that projected out the dorsal acoustic stria. Some of these labeled somata (n=17 out of 58) were contacted by labeled swellings of the commissural axons. Both of the labeled neurons in Figure 7A were contacted by labeled swellings.

DISCUSSION

Radiate Multipolar Cells as a Source of CN Commissural Projection

We describe here new data on the course and terminations of commissural axons that originate from large multipolar neurons of the VCN and perhaps the DCN (Adams and Warr, 1976; Cant and Gaston, 1982; Wenthold, 1987). Our data show a strong relationship between the labeling of these axons and radiate multipolar neurons (Fig. 1B). Radiate neurons of the VCN almost certainly correspond to D stellate cells, which project their axons dorsally (Oertel et al., 1990), as do our labeled commissural axons. Our radiate axon terminals have inhibitory morphology, which fits with previous data that type II cells/D cells/radiate cells/onset units are inhibitory (Wenthold, 1987; Alibardi, 1998, 2000; Kolston et al., 1992; Doucet et al., 1999; Smith et al., 2005). However, since our injection site was in the DCN, there is likely to be some labeling of DCN commissural neurons (which would be obscured by the injection site). The number of these neurons is expected to be small compared to those in the VCN (Shore et al., 1992; Schofield and Cant, 1996; Zhou et al., 2010).

The labeling that results from our DCN injections represents a more homogeneous population than that obtained with large injections encompassing the entire CN. For example, our radiate commissural axons are significantly thicker than auditory nerve fibers, in contrast to axons of planar multipolar cells, which are thinner (Darrow et al. 2012). Almost all radiate commissural axons exit the dorsal acoustic stria (Fig. 3) and all of them terminate primarily in the core of the opposite CN. In contrast, the excitatory system of commissural neurons has neurons with smaller cell bodies and presumably thinner axons, a lower degree of innervation of the soma, and its neurons tend to originate and send terminations to the edges of the CN (Shore et al., 1992; Schofield and Cant, 1996; Doucet et al., 2009; Zhou et al., 2010). Our data are consistent with the idea that excitatory commissural neurons were not labeled by our injections because they lack processes to the DCN. Because other excitatory multipolar cells have such processes (Oertel et al., 1990; Doucet and Ryugo, 2006), this suggests that excitatory commissural neurons differ from type I cells/T cells/planar cells/chopper units in this respect as well as being commissural. Because these neurons were not labeled by our injections, further work will be necessary to confirm this suggestion. Excitatory effects of contralateral sound tend to have long latencies and these effects can be up-regulated following hearing loss (Sumner et al., 2005; Bledsoe et al., 2009).

Axonal Trajectory

The axonal course we describe is similar to that of a few commissural axons from onset chopper units in guinea pig (Arnott et al., 2004) and in cat (Smith et al., 2005), and similar to the course described by extracellular labeling studies in cats (Cant and Gaston, 1982). The axons exit via the dorsal acoustic stria and cross in the dorsal half of the brainstem before entering the opposite CN via various routes. Their course, in some cases close to the floor of the fourth ventricle, suggests that these axons may be unintentionally cut in experiments intending to sever the olivocochlear bundle. The depth of such a cut could be utilized to determine the percentage of commissural axons that are affected; some published micrographs illustrate cuts deep enough to sever all the commissural axons (e.g., Fig. 4 in Rajan and Johnstone, 1989). The effects of loss of the commissural vs. olivocochlear bundles may be difficult to untangle, especially if the metric is generated at central locations or is a behavioral measure (Dewson, 1968; Irving et al., 2011). Lesions of the olivocochlear bundle have been reported to decrease the adjustment of the dynamic range of hearing, the ability to discern signals in noisy backgrounds, and the protection from high-level sounds (reviewed by Ryugo et al., 2011). By contrast, lesions of the commissural system without

accompaniment of other systems have not been reported. In addition, another type of lesion would affect radiate commissural axons: those made by cutting the dorsal acoustic stria. In this case, the loss of the commissural network also might contribute to the post-lesion behavioral changes (May, 2000).

Terminations

Previous results (Cant and Gaston, 1982) on commissural terminations found a widespread distribution throughout the CN, with the densest innervation in the AVCN, the PVCN, and the fusiform and superficial layers of the DCN. Present results are in agreement, and in addition point out a paucity of swellings in the most ventral parts of all subdivisions. In the VCN, the terminations are mainly in the core with a limited projection to edge regions. This is a distribution like that of auditory nerve fibers (Osen, 1970; Fekete et al., 1984) but complementary to CN branches of the olivocochlear neurons, which are mainly to the edges (Osen et al., 1984; Brown et al., 1991). The new data presented in the present study allow comparision of several fiber types that innervate the CN. Compared to an average of 250 swellings/commissural axon, olivococochlear branches to the CN form fewer, about 73 per branch (Brown et al. 1988) in mouse. Auditory-nerve fiber data are not available in mouse, but in cats, there are 25 – 250 swellings per ascending branch, which is the part that runs through AVCN (Liberman, 1991). If physiological action is correlated with the number of swellings, a single commissural axon may have a powerful action compared to these other CN inputs. There are many unknowns tempering this conclusion, including the number of synapses per swelling and the somatic vs. dendritic locations of the synapses. One known fact, however, is that olivocochlear branches run along and form multiple synapses onto single proximal dendrites in the CN (Benson and Brown, 1990), which suggests a focused effect on a small number of targets. In contrast, commissural terminations, like those of auditory nerve fibers, span the CN and would appear to have numerous separate targets, suggesting a much wider functional effect.

We have confirmed earlier suggestions, based on indirect measures, that commissural neurons had large terminal fields (Shore et al., 1992; Schofield and Cant, 1996). Our direct measurements of individual axons show that some terminate over almost the entire dorso-ventral axis of the CN (Fig. 4) but typically kept within a single CN subdivision. This pattern would suggest an effect on processing of almost all sound frequencies over a single subdivision. Those axons with narrower distributions would suggest a more limited action. Physiologically, contralateral tones have diverse patterns of effects in the frequency domain (Davis, 2005; Ingham et al., 2006): some are broad and encompass a large part of the ipsilateral excitatory region, whereas others are narrow and act mostly on the central part. These actions may correspond to the broad vs. narrow terminations shown in the present study. One apparent difference between the anatomical and physiological results is that the commissural terminations are most dense in AVCN, whereas physiological effects appear to be greatest in DCN (Ingham et al., 2006). Physiological effects, however may reflect a variety of descending and other pathways in addition to the commissural pathway (Bledsoe et al., 2009).

The widespread termination of the commissural axons studied here, which is across all subdivisions of the CN, strongly suggests that the targets of commissural axons are diverse. Our results demonstrate that commissural endings form synapses on neurons of at least several types. The results are limited because most synapses observed were onto dendrites, which are difficult to trace with electron microscopy. Previously, labeled commissural endings are reported to be mostly in neuropil, suggesting dendritic terminations, but some abut bushy cells (Cant and Gaston, 1982; Schofield and Cant, 1996). Physiological recordings of CN units reinforce the idea of diverse targets, because contralateral sound influences a variety of unit types in CN as defined by response to sound (Shore et al., 2003;

Ingham et al., 2006). One of the targets of the present study was identified ultrastructurally as a type I multipolar cell, which fits with previous findings that units corresponding to T multipolar cells are commissural targets (Needham and Paolini, 2003). In the present study, the multipolar cell was retrogradely labeled, and thus projected across the brainstem to the DCN injection site by its commissural axon. This finding opens up the possibility that the inhibitory commissural system, whose axons were labeled in our study, can inhibit the excitatory commissural system on the opposite side.

Physiological Effects

The synaptic morphology that we observed, with symmetric junctions and pleomorphic vesicles (Uchizono, 1965), suggests inhibitory effects of the radiate commissural system. Such synaptic morphology has been shown in endings of local collaterals made by inhibitory multipolar cells near the cell body (Smith and Rhode, 1989). Targets of those local collaterals, like those of the commissural axons, are mainly dendrites. Ipsilaterally, D-stellate cells are a prominent source of glycinergic input to T-stellate cells (Ferragamo et al., 1998). This idea fits with the original observation that the radiate commissural pathway is glycinergic (Wenthold, 1987). All of these findings are in harmony with predominant physiological effects of contralateral sound being inhibitory (Mast, 1970; Joris and Smith, 1998; Shore et al., 2003; Ingham et al., 2006).

When might this system be activated? The radiate commissural neurons have an “onset chopper” response to sound (Arnott et al., 2004; Smith et al., 2005), with rate vs. level functions that are almost non-saturating so that their discharge rates are highest at the highest sound levels (Rhode and Smith, 1986; Winter and Palmer, 1995). Their local collaterals may perform the role of the “wideband inhibitor”, which decreases responses to sound over a wide frequency band and enables the central excitatory area to be sharper (Nelken and Young, 1994; Winter and Palmer, 1995). This role may sharpen some of the spectral cues used for sound localization (Davis, 2005). The myelination and thick diameters of the commissural axons should ensure quick spike conduction across the brainstem to the opposite side: Using the 5 mm distance and a conduction velocity of 20 m/s (Sakai and Woody, 1988), an impulse should travel from one CN to the other in about 0.25 ms (in mouse, with larger species having longer times). This short time suggests an action on a quick time scale, consistent with the fast latencies reported for the effects of contralateral sound (Mast, 1970; Babalian et al., 1999; Shore et al. 2003; Needham and Paolini, 2003; Ingham et al., 2006). The radiate commissural pathway may thus be poised for rapidly balancing the inputs on the two sides. This action should be much quicker than that of the lateral olivocochlear system (Darrow et al., 2006), which may provide balance with a slow time course because of its thin, unmyelinated axons.

Acknowledgments

Grant sponsor: National Institutes of Health-NIDCD, grant number DC01089 (to M.C.B.)

We thank Dr. M. C. Liberman for reviewing a previous version of this manuscript. Preliminary results of this study were presented in abstract form at the Association for Research in Otolaryngology Midwinter Meeting, February, 2012.

All authors had full access to all the data in the study and take responsibility for the integrity of the data and the accuracy of the data analysis. Roles of authors: study concept and design: MCB, KND. Acquisition, analysis and interpretation of data: MCB, MD, TEB, KND. Statistical analysis and drafting of the manuscript: MCB. Critical revision of the manuscript, administrative, technical, and material support: MCB, MD, TEB, KND. Study supervision and obtaining funding: MCB.

References

Abramoff MD, Magalhaes PJ, Ram SJ. Image Processing with ImageJ. Biophotonics Intl. 2004; 11:36–42.

Adams JC, Warr WB. Origins of axons in the cat's acoustic striae determined by injections of horseradish into severed tracts. J Comp Neurol. 1976; 170:107–122. [PubMed: 61976]

Alibardi I. Ultrastructural and immunocytochemical characterization of commissural neurons in the ventral cochlear nucleus of the rat. Ann Anat. 1998; 180:427–438. [PubMed: 9795693]

Alibardi I. Cytology, synaptology, and immunocytochemistry of commissural neurons and their putative axonal terminals in the dorsal cochlear nucleus of the rat. Ann Anat. 2000; 182:207–220. [PubMed: 10836094]

Arnott RH, Wallace MN, Shackleton TM, Palmer AR. Onset neurones in the anteroventral cochlear nucleus project to the dorsal cochlear nucleus. J Assoc Res Otolaryngol. 2004; 5:153–170. [PubMed: 15357418]

Babalian AL, Ryugo DK, Vischer MW, Rouiller EM. Inhibitory synaptic interactions between cochlear nuclei: evidence from an in vitro whole brain study. Neuroreport. 1999; 10:1913–1917. [PubMed: 10501532]

Benson TE, Brown MC. Synapses formed by olivocochlear axon branches in the mouse cochlear nucleus. J Comp Neurol. 1990; 295:52–70. [PubMed: 2341636]

Bledsoe SC Jr, Koehler S, Tucci DL, Zhou J, Le Prell CG, Shore SE. Ventral cochlear nucleus responses to contralateral sound are mediated by commissural and olivocochlear pathways. J Neurophysiol. 2009; 102:886–900. [PubMed: 19458143]

Bourk TR, Mielcarz JP, Norris BE. Tonotopic organization of the anteroventral cochlear nucleus of the cat. Hearing Res. 1981; 4:215–241.

Brawer JR, Morest DK, Kane EC. The neuronal architecture of the cochlear nucleus of the cat. J Comp Neurol. 1974; 155:251–300. [PubMed: 4134212]

Brown MC. Fiber pathways and branching patterns of biocytin-labeled olivocochlear neurons in the mouse brainstem. J Comp Neurol. 1993; 337:600–613. [PubMed: 8288773]

Brown MC, Liberman MC, Benson TE, Ryugo DK. Brainstem branches from olivocochlear axons in cats and rodents. J Comp Neurol. 1988; 278:591–603. [PubMed: 3230172]

Brown MC, Pierce S, Berglund AM. Cochlear-nucleus branches of thick (medial) olivocochlear fibers in the mouse: A cochleotopic projection. J Comp Neurol. 1991; 303:300–315. [PubMed: 2013642]

Cant NB. The fine structure of two types of stellate cells in the anterior division of the anteroventral cochlear nucleus of the cat. Neurosci. 1981; 6:2643–2655.

Cant NB, Gaston KC. Pathways connecting the right and left cochlear nuclei. J Comp Neurol. 1982; 212:313–326. [PubMed: 6185548]

Darrow KN, Benson TE, Brown MC. Planar multipolar cells in the cochlear nucleus project to medial olivocochlear neurons in mouse. J Comp Neurol. 2012 In Press.

Darrow KN, Maison SF, Liberman MC. Cochlear efferent feedback balances interaural sensitivity. Nat Neurosci. 2006; 9:1464–1476.

Davis KA. Contralateral effects and binaural interactions in dorsal cochlear nucleus. J Assoc Res Otolaryngol. 2005; 6:280–196. [PubMed: 16075189]

Dewson JH. Efferent olivocochlear bundle: Some relationships to stimulus discrimination in noise. J Neurophysiol. 1968; 31:122–130. [PubMed: 4966613]

Doucet JR, Lenhan NM, May BJ. Commissural neurons in the rat ventral cochlear nucleus. J Assoc Res Otolaryngol. 2009; 10:269–280. [PubMed: 19172356]

Doucet JR, Ross AT, Gillespie MB, Ryugo DK. Glycine immunoreactivity of multipolar neurons in the ventral cochlear nucleus which project to the dorsal cochlear nucleus. J Comp Neurol. 1999; 408:515–531. [PubMed: 10340502]

Doucet JR, Ryugo DK. Projections from the ventral cochlear nucleus to the dorsal cochlear nucleus in rats. J Comp Neurol. 1997; 385:245–264. [PubMed: 9268126]

Doucet JR, Ryugo DK. Axonal pathways to the lateral superior olive labeled with biotinylated dextran amine injections in the dorsal cochlear nucleus in rats. J Comp Neurol. 2003; 461:452–465. [PubMed: 12746862]

Doucet JR, Ryugo DK. Structural and functional classes of multipolar cells in the ventral cochlear nucleus. Anat Rec A. 2006; 288A:331–344.

Fekete DM, Rouiller EM, Liberman MC, Ryugo DK. The central projections of intracellularly labeled auditory nerve fibers in cats. J Comp Neurol. 1984; 229:432–450. [PubMed: 6209306]

Ferragamo MJ, Golding NL, Oertel D. Synaptic inputs to stellate cells in the ventral cochlear nucleus. J Neurophsysiol. 1998; 79:51–63.

Ingham NJ, Bleeck S, Winter IM. Contralateral inhibitory and excitatory frequency response maps in the mammalian cochlear nucleus. Eur J Neurosci. 2006; 24:2515–2529. [PubMed: 17100840]

Irving S, Moore DR, Liberman MC, Sumner CJ. Olivocochlear efferent control in sound localization and experience-dependent learning. J Neurosci. 2011; 31:2493–2501. [PubMed: 21325517]

Joris PX, Smith PH. Temporal and binaural properties in dorsal cochlear nucleus and its output tract. J Neurosci. 1998; 18:10157–10170. [PubMed: 9822769]

Koelle GB, Friedenwald JS. A histochemical method for localizing cholinesterase activity. Proc Soc Exp Biol. 1949; 70:617–622. [PubMed: 18149447]

Kolston J, Osen KK, Hackney CM, Ottersen OP, Storm-Mathisen J. An atlas of glycine- and GABA-like immunoreactivity and colocalization in the cochlear nuclear complex of the guinea pig. Anat Embryol. 1992; 186:443–465. [PubMed: 1443654]

Liberman MC, Oliver ME. Morphometry of intracellularly labeled neurons of the auditory nerve: Correlations with functional properties. J Comp Neurol. 1984; 223:163–176. [PubMed: 6200517]

Liberman MC. Central projections of auditory-nerve fibers of differing spontaneous rates. I. Anteroventral cochlear nucleus. J Comp Neurol. 1991; 313:240–258. [PubMed: 1722487]

Mast TE. Binaural interaction and contralateral inhibition in dorsal cochlear nucleus of chinchilla. J Neurophysiol. 1970; 33:108–115. [PubMed: 5411507]

Needham K, Paolini AG. Fast inhibition underlies the transmission of auditory information between cochlear nuclei. J Neurosci. 2003; 23:6357–6361. [PubMed: 12867521]

Nelken I, Young ED. Two separate inhibitory mechanisms shape the responses of dorsal cochlear nucleus type IV units to narrowband and wideband stimuli. J Neurophysiol. 1994; 71:2446–2462. [PubMed: 7931527]

Oertel D, Wu SH, Garb MW, Dizack C. Morphology and physiology of cells in slice preparations of the posteroventral cochlear nucleus of mice. J Comp Neurol. 1990; 295:136–154. [PubMed: 2341631]

Oertel D, Wright S, Cao X, Ferragamo M, Bal R. The multiple functions of T stellate/multipolar/chopper cells in the ventral cochlear nucleus. Hearing Res. 2011; 276:61–69.

Oliver DL. Projections to the inferior colliculus from the anteroventral cochlear nucleus in the cat: Possible substrates for binaural interaction. J Comp Neurol. 1987; 264:24–46. [PubMed: 2445792]

Osen KK. Cytoarchitecture of the cochlear nuclei in the cat. J Comp Neurol. 1969; 136:453–484. [PubMed: 5801446]

Osen KK. Course and termination of the primary afferents in the cochlear nuclei of the cat. Arch Ital Biol. 1970; 108:21–51. [PubMed: 5438720]

Osen KK, Mugnaini E, Dahl A-L, Christiansen AH. Histochemical localization of acetylcholinesterase in the cochlear and superior olivary nuclei. A reappraisal with emphasis on the cochlear granule cell system. Arch Italiennes de Biologie. 1984; 122:169–212.

Rasmussen GL. The olivary peduncle and other fiber connections of the superior olivary complex. J Comp Neurol. 1946; 84:141–219. [PubMed: 20982804]

Rhode WS, Smith P. Encoding of timing and intensity in the ventral cochlear nucleus of the cat. J Neurophysiol. 1986; 56:261–286. [PubMed: 3760921]

Ryugo DK, Wu MM, Pongstaporn T. Activity-related features of synapse morphology: A study of endbulbs of Held. J Comp Neurol. 1996; 365:141–158. [PubMed: 8821447]

Ryugo, DK.; Fay, RR.; Popper, AN. Auditory and Vestibular Efferents. New York: Springer Science +Business Media, LLC; 2011. p. 359

Sakai J, Woody CD. Relationships between axonal diameter, soma size, and axonal conduction velocity of HRP-filled, pyramidal tract cells of awake cats. Brain Res. 1988; 460:1–7. [PubMed: 2464399]

Schofield BR, Cant NB. Origins and targets of commissural connections between the cochlear nuclei in guinea pigs. J Comp Neurol. 1996; 375:128–146. [PubMed: 8913897]

Shore SE, Helfert RH, Bledsoe SC, Altschuler RA, Godfrey DA. Connections between the cochlear nuclei in guinea pig. Hearing Res. 1992; 62:16–26.

Shore SE, Sumner CJ, Bledsoe SC, Lu J. Effects of contralateral sound stimulation on unit activity of ventral cochlear nucleus neurons. Exp Brain Res. 2003; 153:427–435. [PubMed: 12961054]

Smith PH, Massie A, Joris PX. Acoustic stria: Anatomy of physiologically characterized cells and their axonal projection patterns. J Comp Neurol. 2005; 482:349–371. [PubMed: 15669051]

Smith PH, Rhode WS. Structural and functional properties distinguish two types of multipolar cells in the ventral cochlear nucleus. J Comp Neurol. 1989; 282:595–616. [PubMed: 2723154]

Staatz-Benson C, Potashner SJ. Uptake and release of glycine in the guinea pig cochlear nucleus after axotomy of afferent or centrifugal fibers. J Neurochem. 1988; 51:370–379. [PubMed: 3392532]

Sumner CJ, Tucci DL, Shore SE. Responses of ventral cochlear nucleus neurons to contralateral sound after conductive hearing loss. J Neurophysiol. 2005; 94:4234–4243. [PubMed: 16093339]

Uchizono K. Characteristics of excitatory and inhibitory synapses in the central nervous system of the cat. Nature. 1965; 207:642–643. [PubMed: 5883646]

Wenthold RJ. Evidence for a glycinergic pathway connecting the two cochlear nuclei: An immunohistochemical and retrograde transport study. Brain Res. 1987; 415:183–187. [PubMed: 3304530]

Winter IM, Palmer AR. Level dependence of cochlear nucleus onset unit responses and facilitation by second tones or broadband noise. J Neurophysiol. 1995; 73:141–159. [PubMed: 7714560]

Zhou J, Zeng C, Cui Y, Shore S. Vesicular glutamate transporter 2 is associated with the cochlear nucleus commissural pathway. J Assoc Res Otolaryngol. 2010; 11:675–687. [PubMed: 20574763]

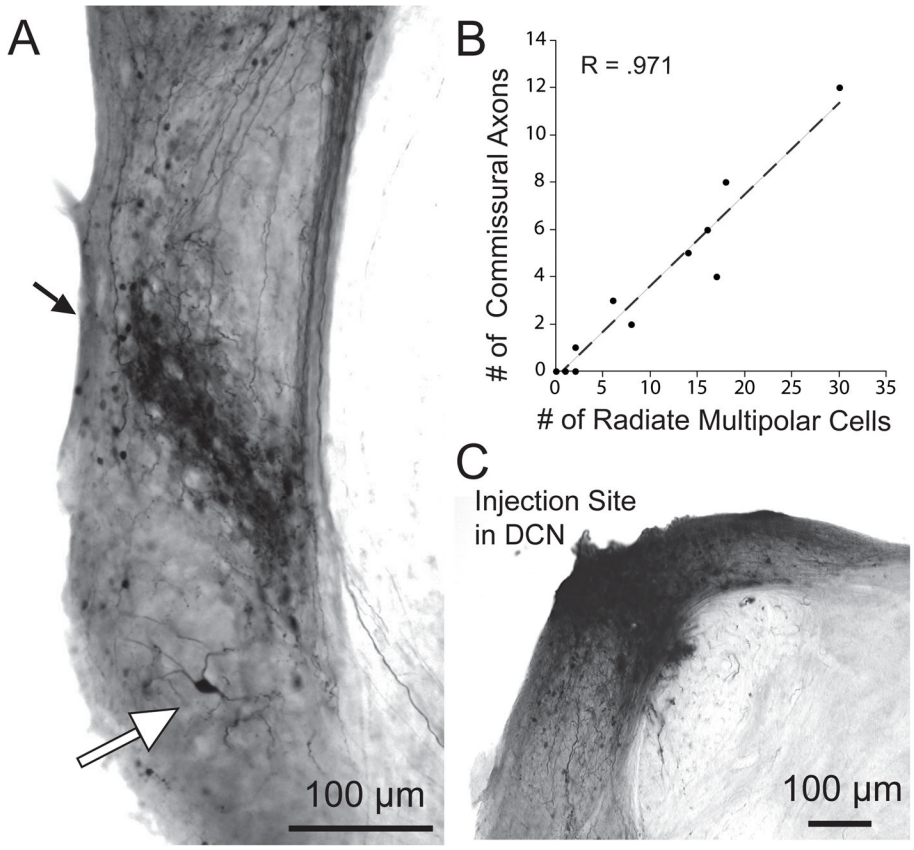

Figure 1.

A: Photomicrograph of labeling in the VCN after an injection of biotinylated dextran amine into the DCN. A narrow band of labeled fibers appears at a middle position within the VCN (black arrow). Some labeled 'planar' neurons are intermixed within this band. The large neuron ventral to this band (white arrow) is identified as a "radiate" multipolar cell because of its long, radiating dendrites. A few small "marginal" multipolar neurons are labeled near the VCN edges. **B:** Plot of the number of labeled commissural axons observed entering the opposite CN as a function of the number of labeled radiate multipolar neurons in the VCN on the side of the injection, in 11 injections with minimal background and dark labeling of multipolar neurons. **C:** Photomicrograph of the injection site.

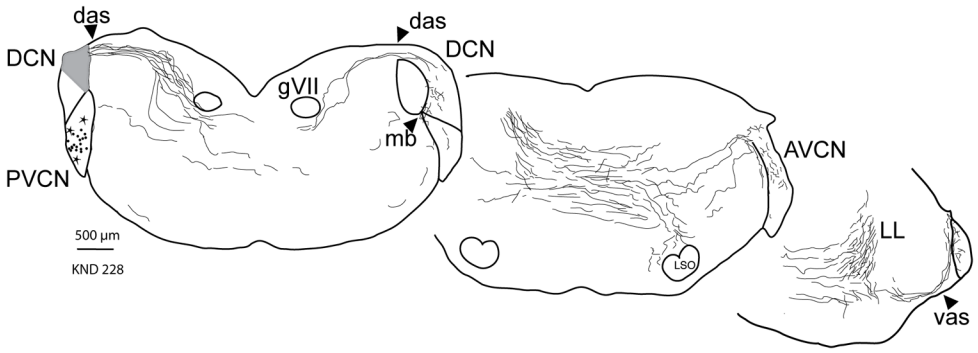

Figure 2.

Atlas drawings showing the labeled fibers from a single large injection site (gray) in the left DCN. Most of the labeled fibers stream out the dorsal acoustic stria (das) and cross the midline to eventually run in the lateral lemniscus (LL) toward the inferior colliculus (not illustrated). Some of these fibers, radiate commissural axons, break off from the main group to innervate the opposite (right-side) CN. They enter via the das, vas, or medial border (mb) between the VCN and the DCN. They terminate within the DCN, posteroventral (PVCN) or anteroventral cochlear nucleus (AVCN) subdivisions. Labeled radiate multipolar neurons (stars) in the VCN of the injected side are the likely source of the commissural axons (Fig. 1B). The more numerous labeled planar multipolar cells (dots) are the source of a different group of labeled fibers that exits the injected CN via the ventral acoustic stria and are not drawn here. Each panel is a composite showing the general pattern in 5 sections (labeling was too heavy for every fiber to be drawn).

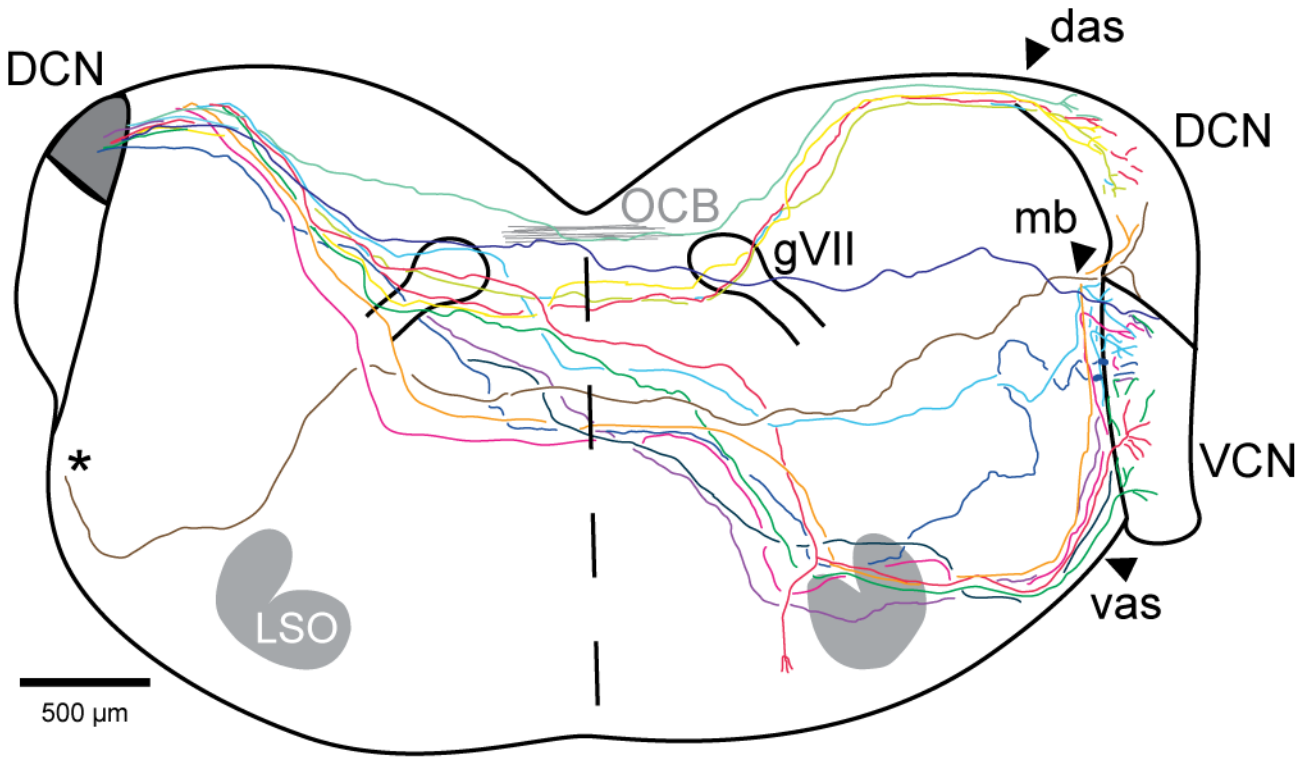

Figure 3.

Camera lucida sketch of the brainstem pathways of 14 single axons labeled in 8 injection cases, overlaid onto a composite brainstem outline (left side of composite is caudal to right side). The axon tracings start within the bundle of labeled fibers near the injection site (shaded) that exit via the das, except for one (*) that traveled out the vas but then ran medially to join the other commissural axons dorsal to the trapezoid body. All the axons cross the midline (dashed line) in the dorsal half of the brainstem and enter into the opposite (right) CN either via its das, vas or mb (same abbreviations as Fig. 2). Gray lines near the dorsal midline indicate the crossing position of the olivocochlear bundle (OCB) as observed in three other brainstems stained for acetylcholinesterase.

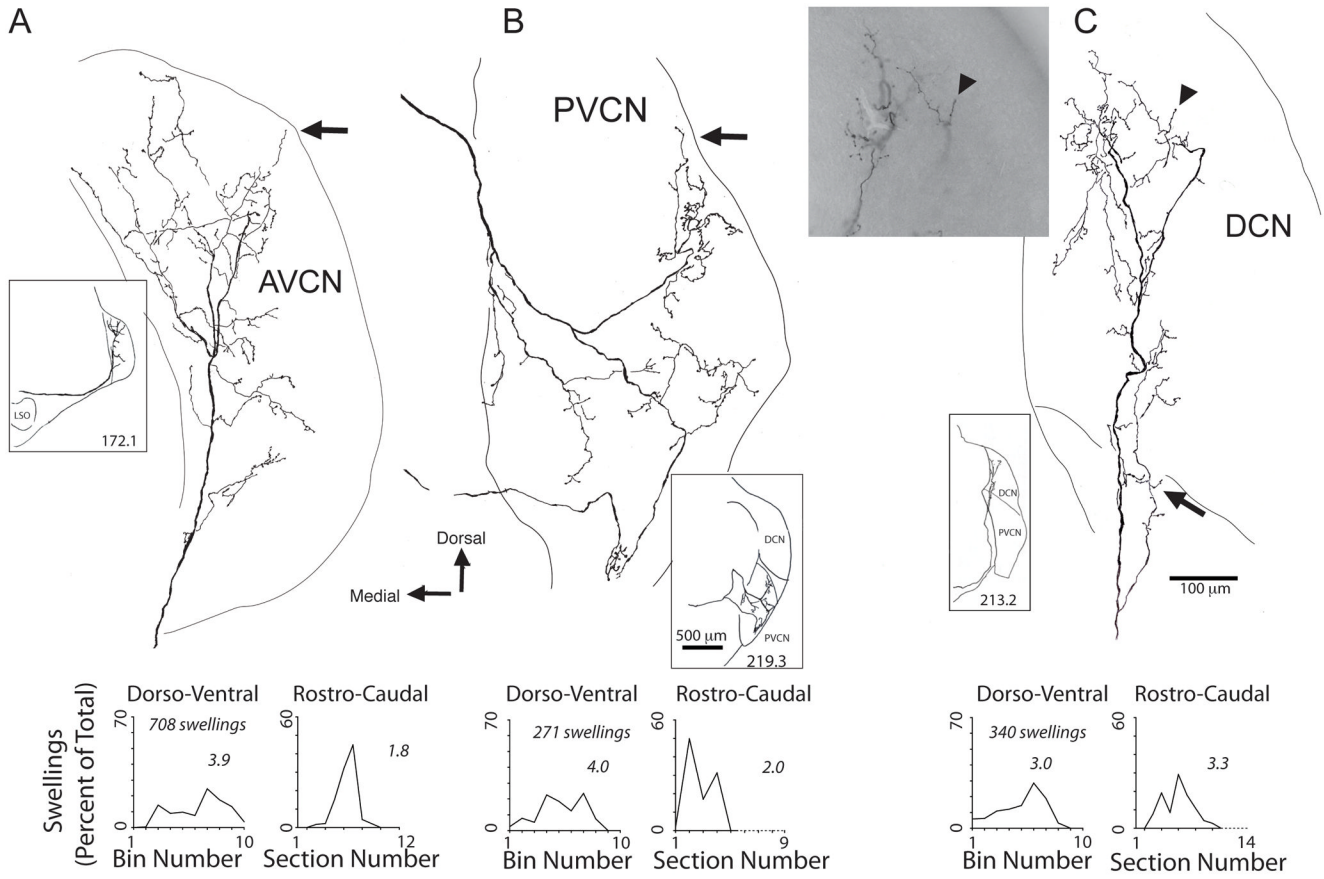

Figure 4.

Camera lucida drawings of three commissural axons, which innervate the AVCN (**A**), PVCN (**B**), or DCN (**C**). Insets show general course of axon at lower magnification. Each pair of graphs below the axon plot the axon's swellings in the dorso-ventral (left plot) and rostro-caudal (right plot) dimensions. Numbers on the plots refer to the 60% extent, a measure of the termination extent (see Methods). In A, the axon terminated mainly in the core of the AVCN with some terminations near its dorsal edge (arrow). In B, the axon formed two branches (inset), both of which were directed to the core of the PVCN with a few endings near its dorsal edge at the granule cell lamina (arrow). In C, the terminations began at the DCN's ventral edge where they were in the deep layers (and arrow shows a few endings that were formed in PVCN near the DCN border). The axon's terminations continued dorsally to the fusiform cell layer (terminal swelling there is indicated by an arrowhead). The same terminal swelling is indicated by another arrowhead in the light micrograph inset, which also shows other branches of the axon in the fusiform cell area.

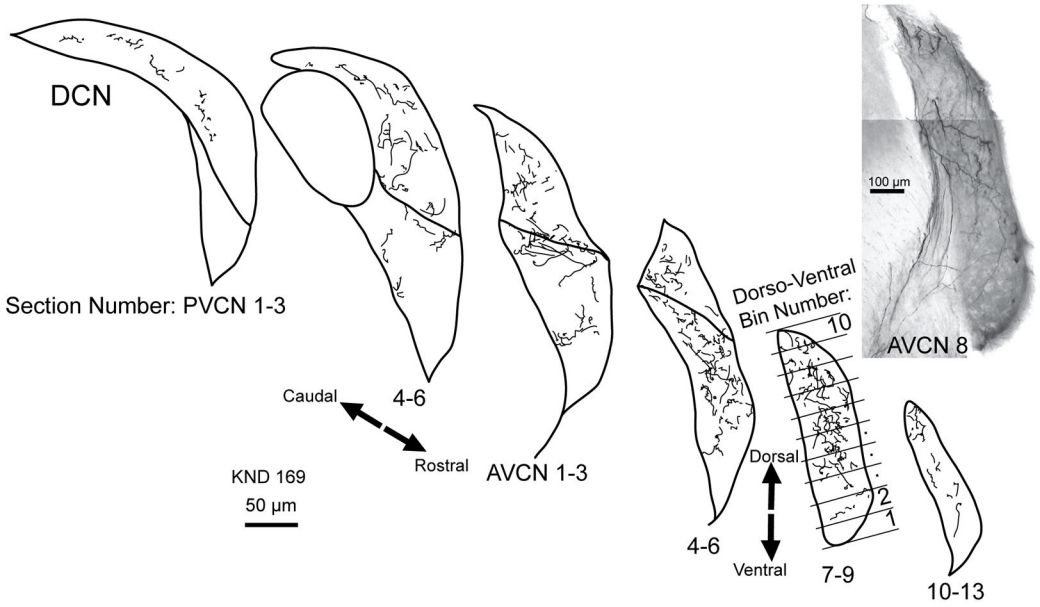

Figure 5.

Atlas drawings of one heavily labeled case, showing commissural axon terminal portions that contain the en passant and terminal swellings. Each atlas drawing represents the labeling in three 80 μm-thick sections. Below are the section numbers for the PVCN and AVCN, which are used for plots in the rostro-caudal dimension (see Fig. 6B and also right plots in each pair on Fig. 4). The bins dividing the CN along its dorso-ventral dimension are illustrated for one drawing (AVCN sections 13–15); these bin numbers are used for plotting in Figure 5A and also left plots in each pair in Fig. 4. At right is a photomontage of labeling in a single section of AVCN. Labeled axons are seen entering the AVCN via the vas.

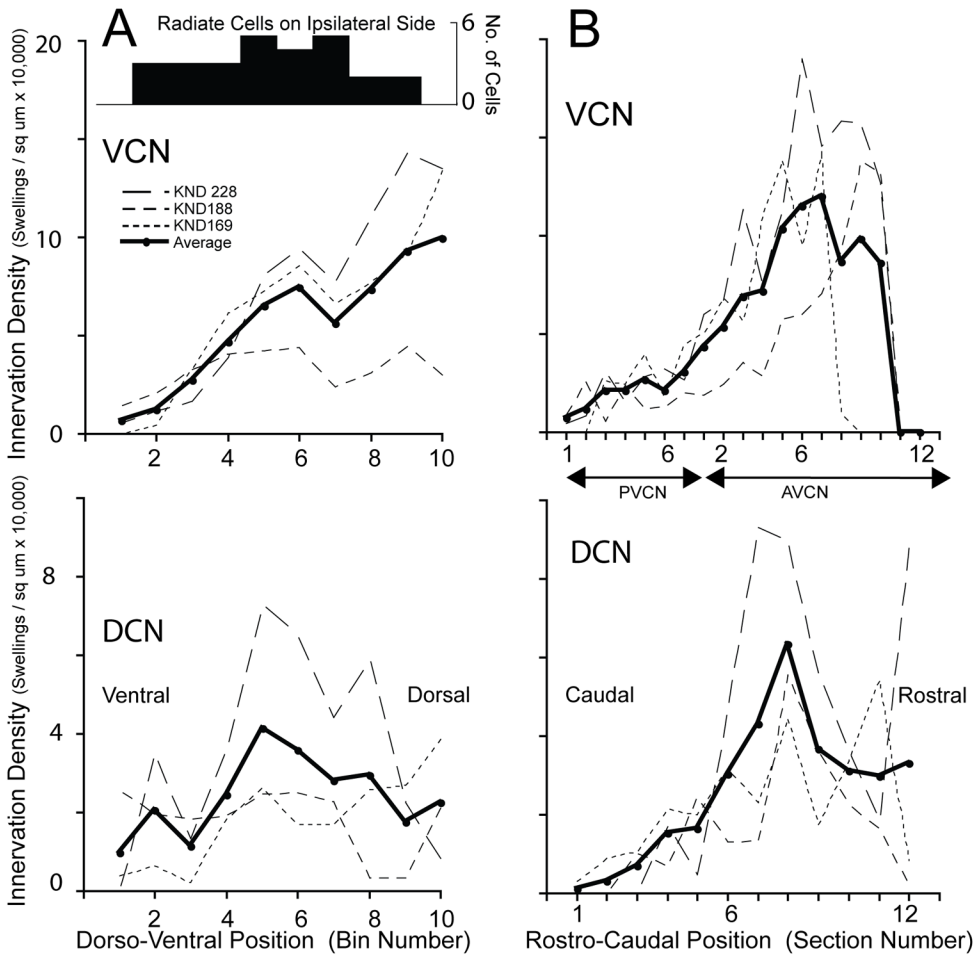

Figure 6.

Plots of innervation density of commissural swellings for three heavily labeled cases (one case illustrated in Fig. 2 and another in Fig. 5). Innervation is plotted separately for the dorso-ventral (**A**) and rostro-caudal (**B**) dimensions. In A, the x-axis dorso-ventral position is in “bin numbers”, which refer to the 10 bins spaced equally along the tonotopic axis of the CN of each section (Fig. 5). In B. the “section numbers” refer to histological sections spaced at 80 μm intervals along the rostro-caudal axis of the CN. Inset in A shows the fairly even dorso-ventral distribution of labeled radiate cells (n=27 total in the three cases) in the VCN on the injected side, which are the presumed source of the commissural fibers.

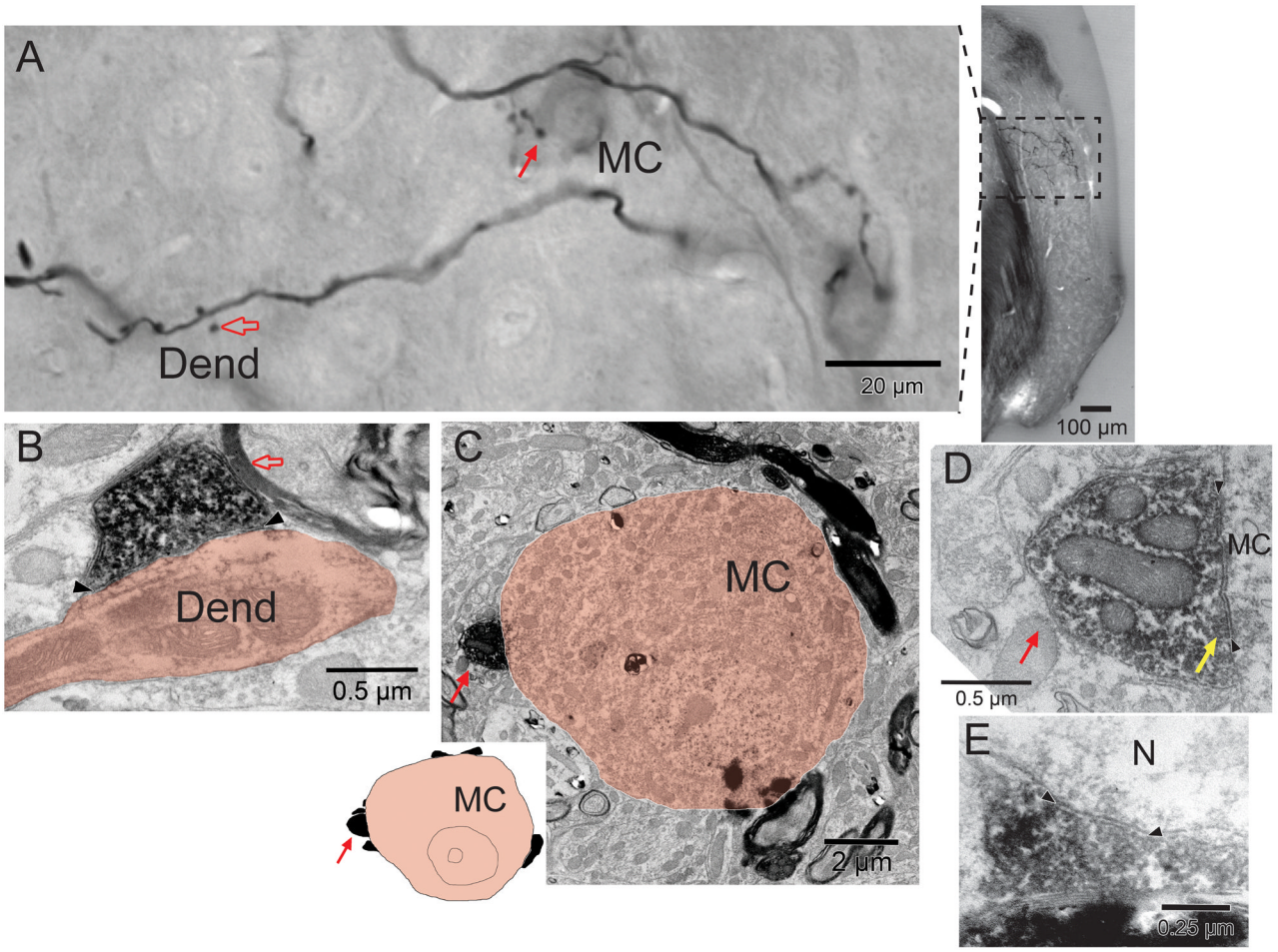

Figure 7.

A: Light micrographs of labeled commissural terminations at high magnification (left, a composite image montage of several focal planes) and lower magnification (right). The axons form numerous en passant swellings, some with short stalks (open arrow) as well as terminal swellings (solid arrow). Terminal swellings contact two neurons (one designated MC because it is a presumed multipolar cell, the other just above the scale bar) that contain faint reaction product perhaps because they are retrogradely labeled. **B–D**: Electron micrographs of material seen in panel A. In B, a synaptic terminal (open red arrow) formed by the en passant swelling in A forms a synapse (arrowheads) onto a dendrite (Dend.). In C, a presumed multipolar cell (MC) receives a terminal (red arrow, and corresponding terminal swelling in panel A). At the top, a labeled myelinated axon passes close to the MC; this axon gave off the branch that ends in the terminal swelling. The MC is of medium size (about 10 µm in this section; about 20 µm in A) and it receives only a few other terminals (20% coverage, inset) suggesting that it is a subtype known as “type I” (Doucet et al., 2009). In D, the terminal is seen in the same section at higher magnification. A synapse (arrowheads) that is formed on the cell body is symmetric because there is minimal postsynaptic material. The synaptic vesicles (yellow arrow) are somewhat obscured by the decoration with reaction product, but are pleomorphic in shape. **E:** Asymmetric synapse (arrowheads) onto an unidentified neurons (N) from another case.